EUROPEAN ORGANIZATION FOR NUCLEAR RESEARCH
CERN-EST

CERN EST/99-006 (SM)

Lowering the activation temperature of TiZrV non-evaporable getter films

A. E. Prodromides, C. Scheuerlein and M. Taborelli

Abstract

In order to reduce the activation temperature of the TiZrV alloy, thin films of various compositions were produced by three-cathode magnetron sputtering on stainless steel substrates. For the characterisation of the activation behaviour the surface chemical composition has been monitored by Auger Electron Spectroscopy (AES) during specific in situ thermal cycles. The volume elemental composition of the film has been measured by Energy Dispersive X-ray spectroscopy (EDX) and the morphology (crystal structure and size of the crystallites) has been investigated by X-ray diffraction (XRD). The criteria indicating the sample quality and its dependence on film structure and chemical composition are presented and discussed.

Keywords: getter, activation, NEG, titanium alloy, vanadium alloy, zirconium alloy, ternary alloys, thin film

Paper presented at the 6th European Vacuum Conference
University Lyon 1, Campus La Doua/IPNL, Lyon, France
7-10 December 1999
To be published in "Vacuum"

Geneva, Switzerland
Décembre 1999

1. INTRODUCTION

In the context of the technical developments for the construction of the Large Hadron Collider (LHC) at CERN, a systematic study has been undertaken in order to produce suitable non-evaporable getter films (NEG). Many coatings composed of various elements have been produced and tested, which all exhibited activation temperature below 400 °C [1,2]. The lowest activation temperature, 200 °C for a 24-hour heating, has been obtained with a TiZrV alloy thin film [3]. A complete review of the results obtained with this coating is presented separately at this conference [4].

In the present study, thin films of titanium-zirconium-vanadium ternaries with various compositions have been produced and characterised by structural and chemical analyses in order to possibly further decrease the activation temperature. Characterisation by surface analytical techniques has been chosen, namely Auger Electron Spectroscopy (AES). It was preferred to other techniques because it results in faster sample production and characterisation.

2. EXPERIMENTAL

2.1 Coating deposition method

NEG thin films are produced by sputtering, because this deposition method provides an easy way to deposit an uniform coating on complex and narrow access chambers, and it can be applied to most metals and their alloys. The initially adopted sputtering system makes use of a composite cathode obtained by twisting together wires of different materials [1]. However, this configuration limits the range of achievable elemental compositions. In order to have a wider choice of compositions a three magnetron sputtering system has been adopted, in which the three cathodes are independently supplied. All our samples have been produced using the same parameters: a total base pressure after bake-out in the 10^{-7} Pa range, an argon discharge pressure of 7×10^{-1} Pa, non heated substrates ($T \leq 90$ °C), water cooled cathodes, constant magnetic fields due to two SmCo magnets (a central Sm_2Co_{17} circular magnet surrounded by a $SmCo_5$ toroidal magnet).

The power applied on each of the targets varies from 20 W to 200 W, with a discharge current between 65 mA and 650 mA and a discharge voltage between 235 V and 410 V. The typical deposition rates are of the order of 0.1 nm/s and the film thickness is about 1 μm. The materials used for the targets are Zr 99.8 %, Ti 99.6 % and V 99.8 %. The type of substrate employed is generally stainless steel 316 LN, excepted for the samples used for thickness measurements which are deposited on glass platelets.

2.2 Characterisation methods

2.2.1 Surface composition analysis by Auger Electron Spectroscopy (AES)

The elemental surface composition as a function of activation temperature was monitored using a special AES apparatus which allows replacing the sample with the analytical head retracted and maintained in an independent vacuum system. For more details see reference [5]. The spectrometer consists of a single-pass cylindrical mirror analyser (PHI 15-110B, Physical Electronics) with a coaxial electron gun. The spectra are acquired in the direct EN(E) mode with a relative energy resolution ΔE/E of 1.2 % (full width at half-maximum). The primary electron energy during the measurements is 3 keV and the primary beam current is typically 1 μA, incident normal to the sample surface. The acquisition of one spectrum lasts about 1 minute (energy range 30 eV-1000 eV, 1 eV step, 20 ms/step, 3 repeats). Since in the present case background

subtraction on the direct spectrum is made difficult by the presence of the lines of Ti, V and O in the same energy range, the spectra are numerically differentiated and the signal intensity is measured as the peak-to-valley height in the derivative spectrum.

The sample holder consists of an OFE copper plate, to which two samples can be clamped by means of four screws so as to provide good thermal contact. The sample plate temperature can be measured by two K-type thermocouples. Heating is achieved by radiation from a filament. The maximum heating temperature which can be reached in this way is 350 °C and the accuracy of the temperature measurement is $\pm$ 3 °C. During sample heating the pressure increases from about 10^{-7} Pa up to $5 \cdot 10^{-6}$ Pa at 350 °C. Electron bombardment is avoided, because the electron stimulated desorption would degrade the vacuum even more.

The surfaces of the NEG alloys are first analysed in the as-received state (after air exposure) and then after in-situ heating for 1 hour at a given temperature. The rate of temperature increase is of 10 degrees per minute. The heating cycle is repeated at 120 °C, 160 °C, 200 °C, 250 °C, 300 °C and 350 °C. Two samples are heated and measured during the same run.

Chemical information can be extracted from the AES spectra of the present samples during activation. In particular the zirconium and carbon line-shape changes provide indications for the degree of activation. Tomita et al. [6] found that the shape of the MNV Zr line correlates with the amount of oxygen adsorbed onto the surface of Zr. A peak at 141 eV grows when the surface gets more and more oxidised and is characteristic for Zr in ZrO_2 . In the present investigation we also find a good correlation between the oxygen KLL intensity and the ratio of the peak-to-valley height of the Zr 147 eV line to the one of the Zr 141 eV peak. Hence the ratio R between the intensity of the metallic Zr peak at 147 eV and the Zr peak at 141 eV, has been chosen as the criterion for the degree of activation of the NEG surface. In other words, a high R value indicates a high degree of activation. Moreover, the calculation of R does not require any previous calibration, normalisation or background subtraction. The disadvantage of this choice is that R can be used only for samples containing zirconium. The chemical modification of the surface while heating is also displayed by the change of the carbon KLL line-shape when adsorbed hydrocarbons produce carbides [7]. However, it is difficult to use these peak-shape changes for monitoring the activation process, since the temperature at which they appear has been found to depend on the amount of C initially present on the surface.

2.2.2 In depth composition analysis by Energy Dispersive X-ray spectroscopy (EDX)

The elemental composition in depth is measured by EDX on a Scanning Electron Microscope (SEM) with an integrated EDX apparatus. Light elements like C and O were neglected in the analysis. The primary electron energy for the analysis is 20 keV. At this energy the analysis depth is slightly larger than the film thickness, as proved by the fact that the signals corresponding to the substrate material can be detected. The values indicated are always in atomic percentages.

2.2.3 Crystal structure and size by X-Ray Diffraction (XRD)

The crystal structure and the size of crystallites are investigated by XRD on the as-received samples. A diffractometer is used in a Θ-2Θ mode, 2Θ varying from 25° to 145° with a 0.01° step and each step lasting for 3 seconds. The X-ray source is a copper anode. The acquisition of XRD spectra is performed either with a Ni filter, or without filter allowing the K_β reflections to be recorded together with the K_α ones.

Under the assumption of a homogeneous single phase and of roughly equiaxed crystal grains, the Scherrer formula $\Delta(2\Theta)=0.88\lambda/(\omega.\cos\Theta)$ is applied to determine the average dimension ω of the crystallites, where λ is the wavelength of the source - i.e. 0.154 nm for copper K_α -, 2Θ is the measured angle in radians and $\Delta(2\Theta)$ is the full width at half maximum in radians.

3. RESULTS

The derivative AES spectra in Fig. 1 are a representative example showing the surface composition variation of a TiZrV film during the activation process. The oxygen line at 512 eV exhibits a strong decrease in intensity going from the as-received spectrum to the 250 °C spectrum, as expected for a reduction of the surface oxide. (Note that the oxygen KLL line and the vanadium LVV line overlap; however, the latter is much smaller than the oxygen line for the surface composition presented in Fig. 1 and is neglected in the discussion.) By going to lower kinetic energy on the spectrum, the next line showing modifications due to heating is the carbon transition at about 270 eV. The change of line-shape indicates that the adsorbed hydrocarbons transform in carbides. The direct spectra (not shown) demonstrate that the strong increase in the peak-to-valley intensity of the derivative between 160 °C and 250 °C is only due to the change in the line-shape and not to a real increase of the carbon coverage. A chlorine peak intensity (181 eV) appears at 200 °C and increases continuously with the increasing temperature. This element is known to segregate to the surface of refractory metals like titanium [8]. As expected the line-shape of the zirconium peak around 141 eV changes upon thermal treatment and already after heating at 160 °C a second structure at 147 eV develops. Again this indicates a reduction of the oxide layer. No traces of elements belonging to the substrate were detected, suggesting that the film is free of large uncoated areas.

In Fig. 2 the AES results for all samples are shown on a ternary diagram as a function of their composition measured by EDX. The activation criterion (R ratio Zr147 eV/Zr141 eV) described above is applied to each sample, for each temperature of the thermal treatment. According to their R value at 200 °C the samples are separated in two groups, i.e. those which exhibited a R value above a threshold and the others. The sharpest difference between the various samples is found at 200 °C and for R = 0.5. At higher temperatures (250 °C) most of the samples are already almost completely metallic and at lower temperature (160 °C) most of them just start to be reduced so that no distinction is possible. Samples which do not contain Zr are also included in Fig. 2. Their state of oxidation is estimated from the evolution of the oxygen intensity in comparison with the samples containing zirconium. They all unambiguously belong to the category of samples which do not exhibit traces of activation at 200 °C. Fig. 2 can be considered as a quality-composition map for the activation temperature of the samples.

Two kinds of film morphologies can be distinguished using Θ-2Θ XRD analysis. Two spectra are representative for each morphology (Fig. 3): in spectrum “a”, a broad peak around 38° is present whereas in spectrum “b” a sharp diffraction peak of the film at 36° can be distinguished. In both cases no other peaks are observed at larger diffraction angles, excepted those of the stainless steel substrate. Under the assumption that the sample is constituted of a single ternary phase, the position of the peaks corresponds to the values predicted by Végard’s law. This law states that the lattice parameter of a crystal is an average of the lattice parameters of each of the constituting elements weighted by the respective atomic concentration. In spite of the fact that Végard’s law can only be applied for similar crystal lattices, examples of applications to hcp and bcc lattices, as for Ti and V, have been reported on the entire mixing range of the elements [9]. The Végard’s law is applied to the Ti-Zr-V alloys using the EDX data for the composition.

Two main groups of samples are found, depending on the grain size: polycrystalline films, with crystallites size over 100 nm (Fig. 3b), and nanocrystalline films with crystallites size

between 3 and 5 nm (Fig. 3a). Two films did not reveal any diffraction peak with the sensitivity of the present measurements and appear to be amorphous at the resolution scale of the XRD. The XRD results are summarised as a function of the sample composition on a Ti-Zr-V ternary diagram in Fig. 4.

4. DISCUSSION

The composition dependence of the activation behaviour was also demonstrated by Meli et al. [10] using XPS on four ternary ZrVFe alloys. In that case, the samples investigated were all crystalline bulk materials. On TiZrV coatings produced by a cathode made by intertwisted wires at CERN, the reduction of the surface oxide layer has already been observed by XPS after heating at 250 °C during 2 hours [3]. For an identical thermal treatment, the reduction was less effective for TiZr, in agreement with the present findings.

One can ask when the onset of the pumping action as a function of the oxidation state of the various metals on the surface takes place. Previous investigations on $Zr_{57}V_{36}Fe_7$ (St707 of SAES Getters) [11, 12] indicate that the surface might already exhibit metallic active sites at temperatures at which Zr is not yet completely reduced. Indeed, both investigations [11, 12] showed by XPS that V is the first element to be reduced upon thermal treatment, quite before Zr. At the resolution used in the present study AES can monitor the reduction of Zr but not of Ti and V. The previous observations [11, 12] enable predicting that a pumping action may set in before Zr is completely reduced.

The structure of the TiZrV films as a function of composition (Fig. 4) shows that, with the noteworthy exception of ZrV samples, the presence of the three elements is necessary in order to obtain nanocrystalline morphology. The nanocrystalline layers present a single phase at the level of sensitivity of these measurements. However, in the range of composition of the nanocrystalline films the ternary phase diagram at room temperature predicts the existence of at least two phases, a bcc β-phase containing Ti, Zr and V and a bcc δ-phase containing Zr dissolved in V [13]. It is likely that the nanocrystalline samples in Fig. 4 represent metastable phases, made possible by their deposition by sputtering. Comparing the representations on Fig. 2 and Fig. 4, a strong correlation between structure and activation behaviour clearly appears. All the getters considered as easily activated (O in Fig. 2) have a nanocrystalline structure (Δ in Fig. 4). Since the solubility and the diffusion coefficient for oxygen are the main quantities which define the activation behaviour, the shown correlation between activation behaviour and crystal size provides direct evidence of the influence of the nanocrystalline structure on the oxygen solubility or/and diffusivity.

5. CONCLUSIONS

The data obtained from the present experiment show clear differences in the activation behaviour of TiZrV thin films depending on the concentration of the three elements. The R ratio calculated for the Zr Auger line enables us to classify the samples investigated so far into two groups. To refine the distinction within these groups further, experiments with finer temperature steps in the thermal treatment will be performed. The validity of the R criterion adopted here will be verified from a functional point of view by pumping speed measurements. This will allow correlating the surface composition evolution with the gettering properties. A clear relation was found between the size of the grains in the films and their activation behaviour. The nanocrystalline structure seems to be necessary to achieve low activation temperatures in this system. The stability of this peculiar morphology against thermal treatment will be investigated, since it is a crucial issue for a practical use of thin film getter coatings.

Acknowledgments

It is a pleasure for us to thank C. Benvenuti, P. Chiggiato and F. Lévy for helpful suggestions and discussions. The three cathode sputtering system has been designed by S. Calatroni and V. Rouzinov. The XRD measurements and interpretations were performed by M. Fassone and S. Sgobba and EDX analysis by G. Jesse and S. Marsh. One of the authors (A. Prodromides) acknowledges the financial support of the Swiss National Foundation for Scientific Research, Project Nr 21-54178.98.

References

[1] C. Benvenuti, P. Chiggiato, F. Cicoira and Y. L'Aminot, *J. Vac. Sci. Technol*. A **16**, 148, (1998)

[2] C. Benvenuti, P. Chiggiato, F. Cicoira and V. Ruzinov, *Vacuum* **50**, 57 (1998)

[3] C. Benvenuti, J.M. Cazeneuve, P. Chiggiato, F. Cicoira, A. Escudeiro Santana, V. Johanek, V. Ruzinov and J. Fraxedas, *Vacuum*, **53**, 219 (1999)

[4] C. Benvenuti , P. Chiggiato, P. Costa Pinto, A. Escudeiro Santana, T. Hedley, A. Mongelluzzo, V. Ruzinov and I. Wevers, Proceedings of EVC-6, Lyon 1999

[5] C. Benvenuti, R. Cosso, J. Genest, M. Hauer, D. Lacarrere, A. Rijllart and R. Saban, *Rev. Sci. Instrum.*, **69**, 2788 (1996)

[6] M. Tomita, T. Tanabe and S. Imoto, *Surf. Sci*. **109**, 173 (1989)

[7] H. J. Mathieu, J. B. Mathieu, D. E. McClure and D. Landolt, *J.Vac.Sci.Technol*. 14, 1023, (1977)

[8] M. Jobin, M. Taborelli and P. Descouts, *Appl.Surf.Sci.* **72**, 363 (1993)

[9] V. D. Dobroel'skii, S. M. Karal'nuk and A. V. Koval', *Metallofizika, Kiev* (Akademiya Nauk Ukrainskoi SSR Institut Metallofiziki) **41**, 73 (1972)

[10] F. Meli, Z. Sheng, I. Vedel and Schlapbach L., *Vacuum* **41**, 1938 (1990)

[11] M. Sancrotti and G. Trezzi, *J. Vac. Sci. Technol*. **A 9**, 182 (1991)

[12] K. Ichimura, M. Matsuyama and K. Watanabe, *J. Vac. Sci. Technol*. **A 5**, 220 (1987)

[13] A. Novikow and H. G. Baer, *Zeitschrift Metallkunde*, **49** 195 (1958)

Figures

Figure 1: Derivative Auger electron spectra of a TiZrV sample showing the evolution of the surface composition during thermal treatment. Note the decrease of the oxygen peak (512 eV) and the increase of the metallic zirconium peak (147 eV) consequent to sample heating. The 1.2 μm thick film, with an in-depth composition of 57 % Zr, 22 % V and 21 % Ti as determined by EDX, is deposited on stainless steel.

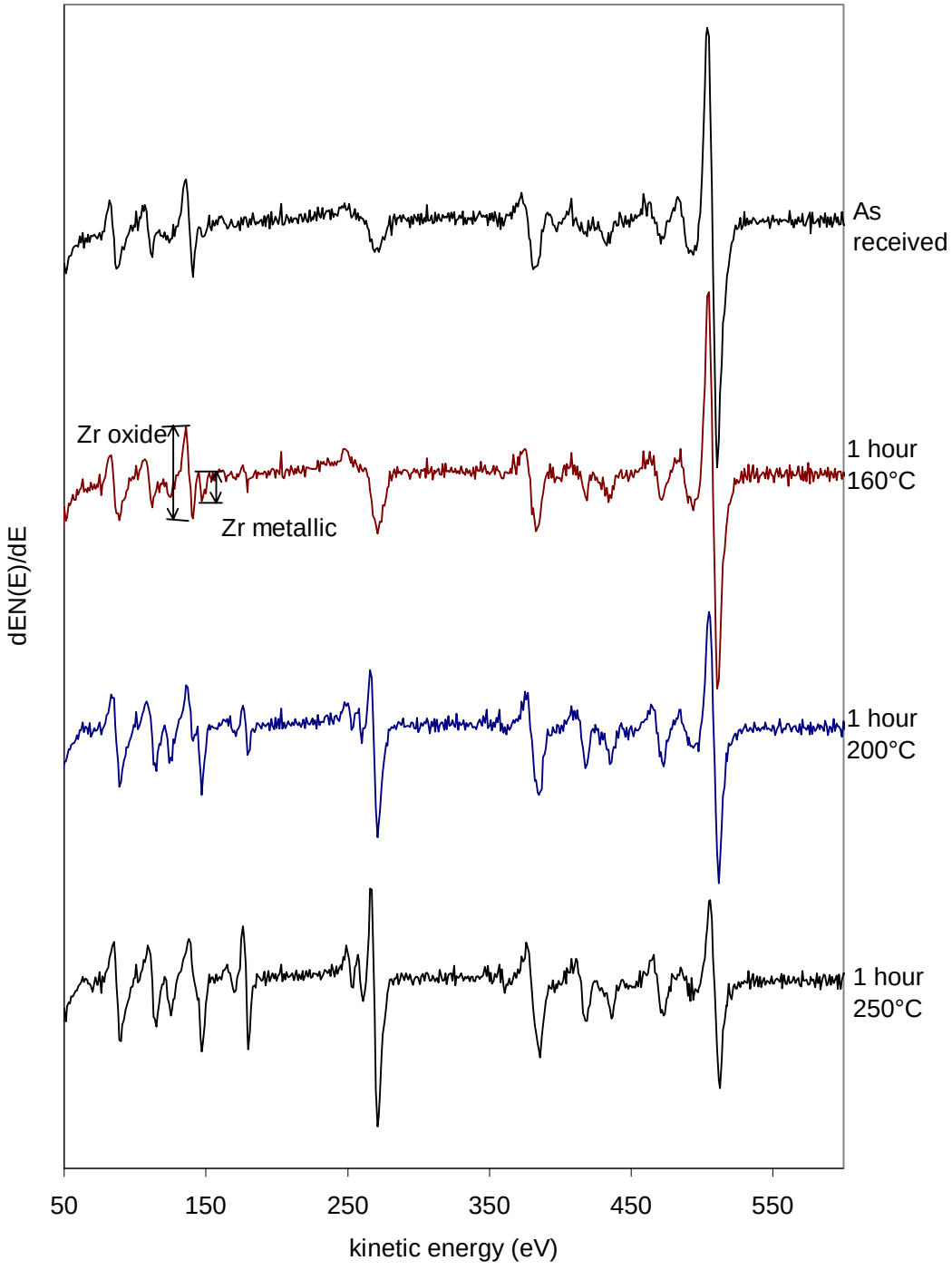

Figure 2: Quality-composition map of Ti-Zr-V films based on the “R criterion” as a function of the in depth elemental composition. The samples with R>0.5 after 200 °C heating for 1 hour are indicated by O and the others by ●.

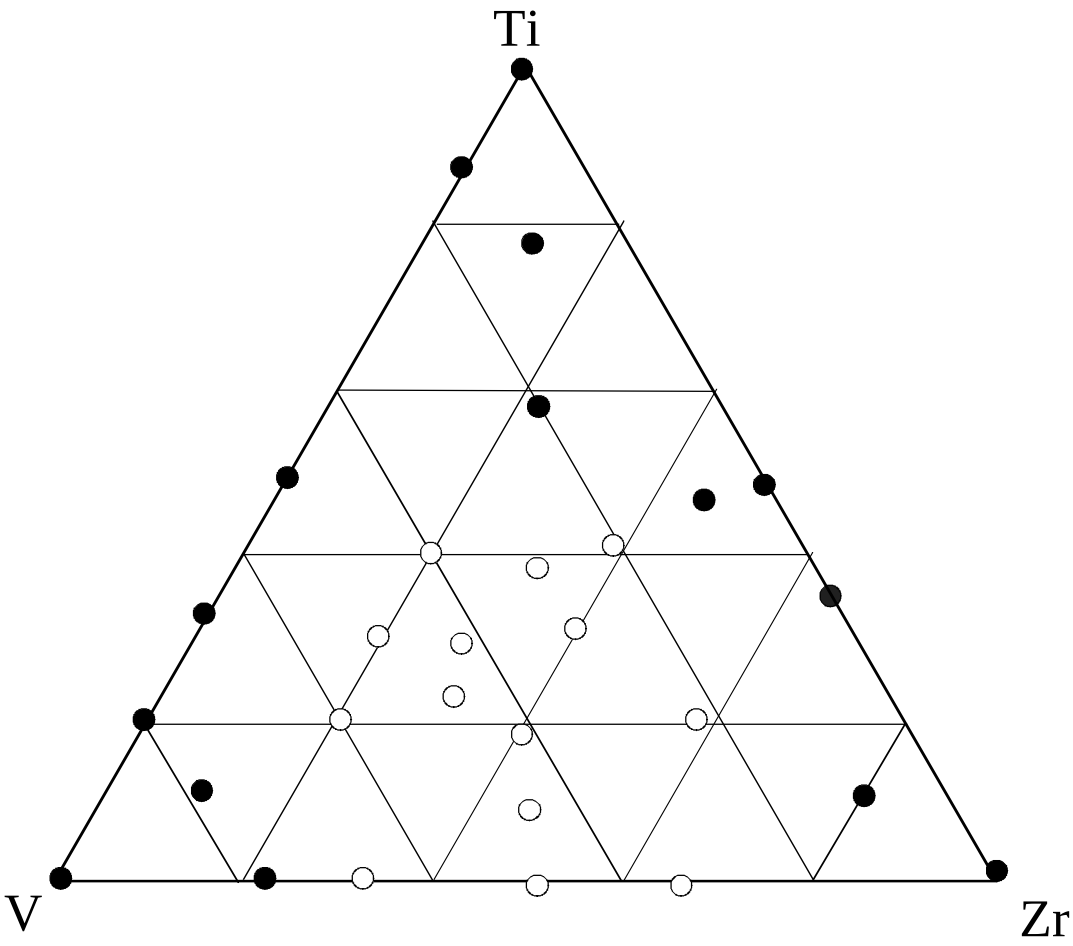

Figure 3: XRD spectra of two TiZrV thin films measured with the same acquisition time. The broad peak of spectrum "a" (Cu K_α source) measured at $\Theta \approx 38°$ for $Ti_{19}Zr_{35}V_{46}$ is typical of the nanocrystalline structure. The sharp peaks in spectrum "b" at $\Theta \approx 36°$ (Cu K_α and K_β source) correspond to the <002> reflections of the well crystallised film of $Ti_{10}Zr_{80}V_{10}$. The peaks marked with • originate from the stainless steel substrate.

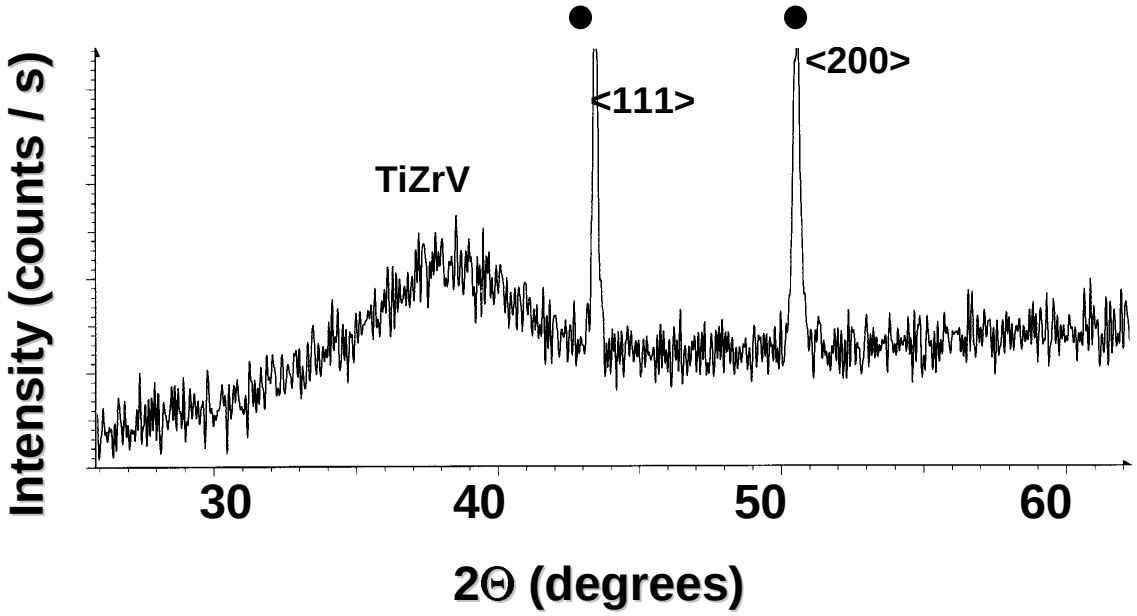

Figure 3 (a)

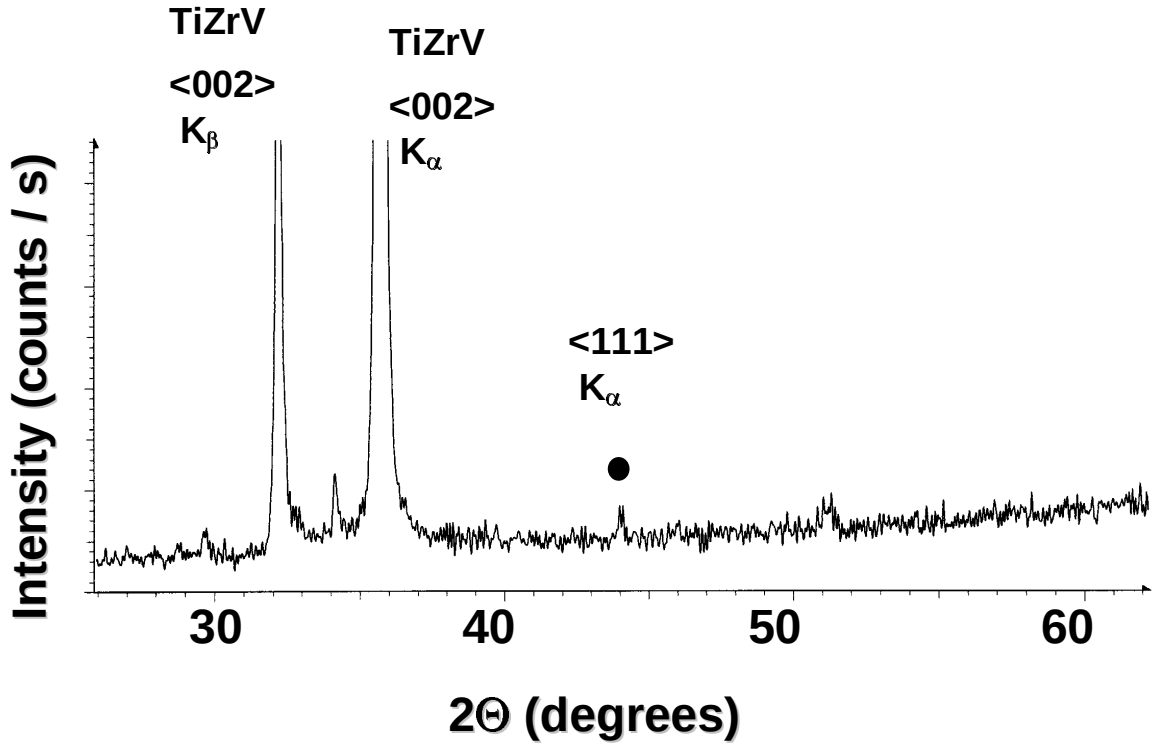

Figure 3 (b)

Figure 4: Map of the crystalline structure of the TiZrV films as a function of their elemental composition. Black triangles ▲ represent the samples with grains larger than 100 nm, empty triangles Δ represent nanocrystalline samples (grains of 3 to 5 nm) and stars * represent samples where no XRD reflections are found.